Author for correspondence:
Hongquan Zhu,
E-mail: zhuhongquan@tsinghua.org.cn

CAMBRIDGE
UNIVERSITY PRESS

A Ka-band high-isolation waveguide power divider with planar output ports and out-of-phase

Cong Tang[1,2] , Xin Gao[1], Hongquan Zhu[1] and Jinrong Zhang[1]

[1]Department of Telemetry and Telecommand, Beijing Institute of Tracking and Telecommunication Technology, Beijing, P. R. China and [2]Southwest China Institute of Electronic Technology, Chengdu, P. R. China

Abstract

A waveguide power divider based on ridge waveguide to microstrip line transition is presented in this paper. To improve the isolation performance, a probe insulator is inserted into the contact face from the center of the waveguide side wall, also two chip resistors are mounted on a planar substrate and connected with the probe to absorb the coupled energy. The impedance transformation is accomplished by ridge waveguide to microstrip line transition, which is hidden in the waveguide. This proposed power divider shows merits of waveguide power dividers and substrate-integrated waveguide power dividers simultaneously, i.e. planar output ports, compact size, and high isolation. For verification, a power divider operating at the Ka-band is simulated, fabricated, and measured. The obtained results show the return loss and isolation are better than 10 and 20 dB, respectively. The measured insertion loss is <1.5 dB, including the insertion loss of waveguide to microstrip line transitions at the output port in the range of 34.6–39 GHz.

Introduction

Power dividers are essential circuits in modern wireless systems such as radar systems, commercial communications, and satellite communications. Various power dividers with small size based on microstrip line structures have recently been reported [1–3]. However, as the operating frequency has increased, e.g. at millimeter-wave frequency band, microstrip line power dividers suffer from high insertion loss. Waveguide power dividers have the merits of high-power capability, good heat-sinking, and so on. Substrate-integrated waveguide (SIW) power dividers show advantages of compact size, and easy connection with planar circuits. Recently, a great number of waveguide and SIW power dividers have been developed.

It is well known, reciprocal lossless T-junctions, including bifurcated waveguide, magic-T, and waveguide T-junctions, are inherently mismatched. So, additional approaches should be developed to obtain good performance at all ports. In the *E*-plane bifurcated waveguide power divider design [4], a resistive film was placed in the *E*-plane to improve the isolation performance. Similarly, an SIW power divider with the same design concept was proposed in [5]. A magic-T has four arms which are mostly located in four different directions. Matching elements, like a cone, wedge, pin, and iris were used to achieve port matching. In [6], a broadband waveguide magic-T junction is presented. A multi-stepped, off-centered conducting cone was optimized by genetically swarm optimization technique to expand the bandwidth. In [7], a magic-T with four arms in the same plane was proposed. The *E*-plane port matching was achieved by a stepped-impedance waveguide transformer and the *H*-plane port is realized by a microstrip impedance transformer. Similarly, a magic-T with coplanar arms was developed in [8]. The *H*-plane sum port was realized by a ridge waveguide coupling structure. The two difference ports were realized by two half-height waveguides. And the corner cut was especially shaped to improve the return loss performance. However, the transition between the coaxial and half-height waveguide narrowed the operating bandwidth.

For the traditional waveguide T-junction, it is the most common waveguide power splitter with the advantages of small size, wide bandwidth, low insertion loss, and easy fabrication, but the isolation performance between two output ports should be improved. So far, many kinds of waveguide T-junctions were investigated. In [9], a planar waveguide T-junction power divider with equal-amplitude, anti-phases, and full bandwidth was presented. Three-stepped-impedance transformer and some ridges were added between the coupling cavity and each port to expand the operation bandwidth. However, no measures were taken to improve the isolation performance. In [10], a waveguide T-junction power divider with good performance was proposed. Isolation between two output ports was realized by introducing a metallic strip probe into the center of the T-junction, the energy coupled by the probe is absorbed by a matched load. Two power dividers which share this similar design concept were proposed in [11, 12]. In [13], a waveguide power divider was realized by
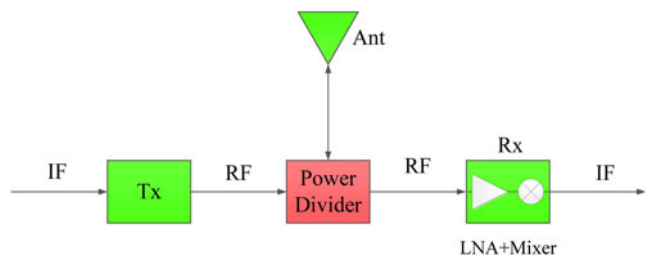
Fig. 1. Block diagram of an FMCW system using the proposed power divider.

Fig. 2. Configuration of the proposed power divider.

properly arranging the configuration and dimensions of the coupling region to control the propagation constants of TE10 and TE30 modes. There was no resistive material between two output ports, and the isolation was realized by two waveguides adjacent to the input port. An SIW power divider which shares a similar design strategy was presented in [14].

Except in [12], the output ports of the waveguide power dividers mentioned above are waveguide. Therefore, additional transition between waveguide and planar transmission line is needed to connect other planar circuits, which will increase the insertion loss and complexity of the circuits. Moreover, although the output ports of the SIW power dividers [15, 16] are planar, the isolation is not high, which restricts its applications in some areas.

In this paper, a high-isolation power divider with waveguide input port and two planar output ports is presented. It shows the merits of planar output ports, high isolation, and compact size. It can be utilized in a short-range frequency-modulated continuous wave (FMCW) system depicted in Fig. 1, as the proposed power divider shows three distinct advantages as follows:

(1) The isolation performance of the proposed power divider is much higher than the conventional circulator whose isolation may not satisfy certain system requirement.
(2) Based on the proposed vertical transition between ridge waveguide and microstrip line, the planar microstrip antenna array can be integrated with the waveguide port of the proposed power divider directly, resulting in a higher system integration level.
(3) Because the output ports are planar, active devices such as PA and low noise amplifier (LNA) in Tx and Rx channels can connect directly with port 2 and port 3, respectively, further improving the system integration level.

In Fig. 1, the traditional circulator is substituted by the proposed power divider. The Tx signal leaked into LNA through the isolation path is utilized as the local oscillator (LO) signal of the single-ended mixer whose LO signal is fed into the same port with radio-frequency signals.

Analysis of the proposed power divider

Figure 2 depicts the configuration of the proposed power divider. It consists of a standard WR-28 waveguide as the input port, two microstrip line output ports, and an insulator. The ridge waveguide, function as an impedance transformer between waveguide and planar transmission line, is hidden in the standard waveguide, so the whole circuit size is more compact than the circuit in [10–12] in which the impedance transformation is accomplished by
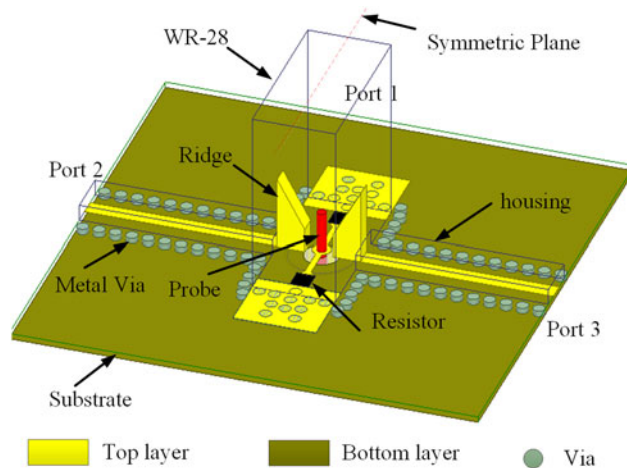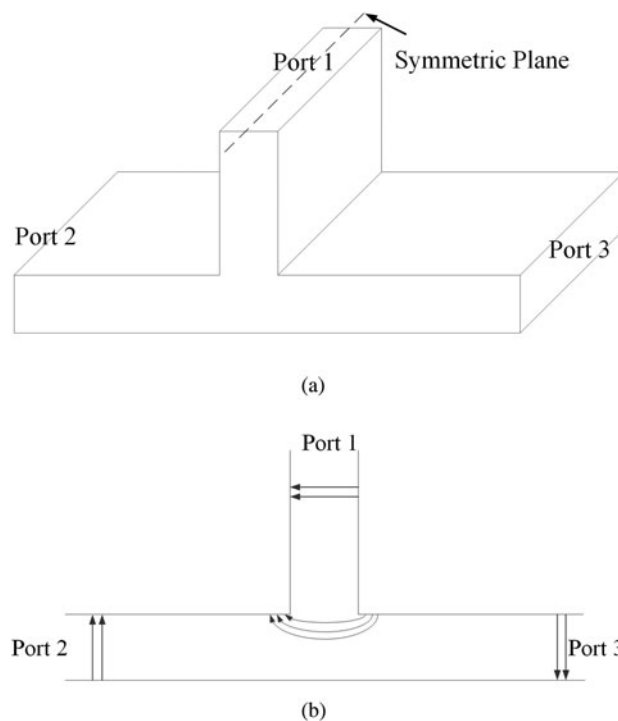

Fig. 3. Structure of the waveguide *E*-type T-junction: (a) structure and (b) electric field distribution.

stepped-impedance waveguide. The isolation between two output ports is realized by an insulator which is inserted into the junction from the bottom of the substrate. Two chip resistors connect with the insulator by two microstrip lines which are also hidden in the waveguide, whereas the isolation circuits in [7, 8, 10–13] are exposed outside which results in a large circuit size. The substrate used in this circuit is Rogers RT/Duroid 5880 with a thickness of 0.254 mm, loss tangent of 0.0009, and relative dielectric constant of 2.2.

The proposed power divider is developed from waveguide E-type T-junction, so its operational principle can be explained by waveguide E-type T-junction. Figure 3 shows the structure of the waveguide E-type T-junction, the electric field of the propagated TE10 mode is depicted in Fig. 3(b). It is well known that

the signal can be propagated only when the electric field direction on the rectangular waveguide wide side is opposite. When ports 2 and 3 are fed by the same amplitude and in-phase signal sources (even-mode excitation), the rectangular waveguide TE10 mode in port 1 cannot be excited under this condition. Thus, there is no signal transmitted to port 1. However, the energy can be coupled to the probe and then be absorbed by chip resistors, thus good isolation can be obtained. When the two output ports are fed by signal sources with equal amplitude and anti-phase (odd-mode excitation), the rectangular waveguide TE10 mode in port 1 is excited under this condition, and no energy is absorbed by chip resistors as the energy coupled to the probe is canceled with each other, resulting in most of the energy is delivered to port 1. According to the analysis above, the scatter parameters of the power divider can be summarized as

$$[S] = \frac{\sqrt{2}}{2} \begin{bmatrix} 0 & -1 & 1 \\ -1 & 0 & 0 \\ 1 & 0 & 0 \end{bmatrix} \quad (1)$$

According to the even- and odd-method [17], the S-parameters of this proposed power divider can be expressed as

$$|S_{11}| = |S_{11}^o| = |\Gamma_{o1}| \quad (2)$$

$$S_{21} = S_{31} = \sqrt{\frac{1 - |\Gamma_{o1}|^2}{2}} \quad (3)$$

$$S_{22} = S_{33} = \frac{\Gamma_{e2} + \Gamma_{o2}}{2} \quad (4)$$

$$S_{23} = \frac{(\Gamma_{e2} - \Gamma_{o2})}{2} \quad (5)$$

where Γ_{o1} and Γ_{o2} are the reflection coefficients at ports 1 and 2 when the whole circuit is under odd-mode excitation, respectively. Γ_{e2} is the reflection coefficient at port 2 when the whole circuit is under the even-mode excitation.

Vertical transition between waveguide and microstrip line

As shown in equation (2), it can be seen that matching at port 1 is determined by the odd-mode reflection coefficient which is mainly determined by the dimensions of the ridge waveguide. Figure 4 shows the physical dimension of the ridge waveguide to microstrip line. For the simplicity of design, the ridge waveguide has the same width as the microstrip line. The microstrip line is surrounded by housing with waveguide modes free and mechanical protection. The inner dimension of the housing is chosen as 0.7 mm × 2 mm. Under this shielding house, the width of 50 Ω transmission line is 0.75 mm. To achieve a good impedance matching over broad frequency band, stepped ridge waveguide is applied. The triangle shape of the ridge waveguide used in this circuit is for the fabrication concern. Figure 5 depicts the simulated results of the return loss of port 1 when $h_1 = 0.78$ mm and h_2 changes. It shows that the ridge height has a great impact on the return loss of port 1, validating the equation in (2).
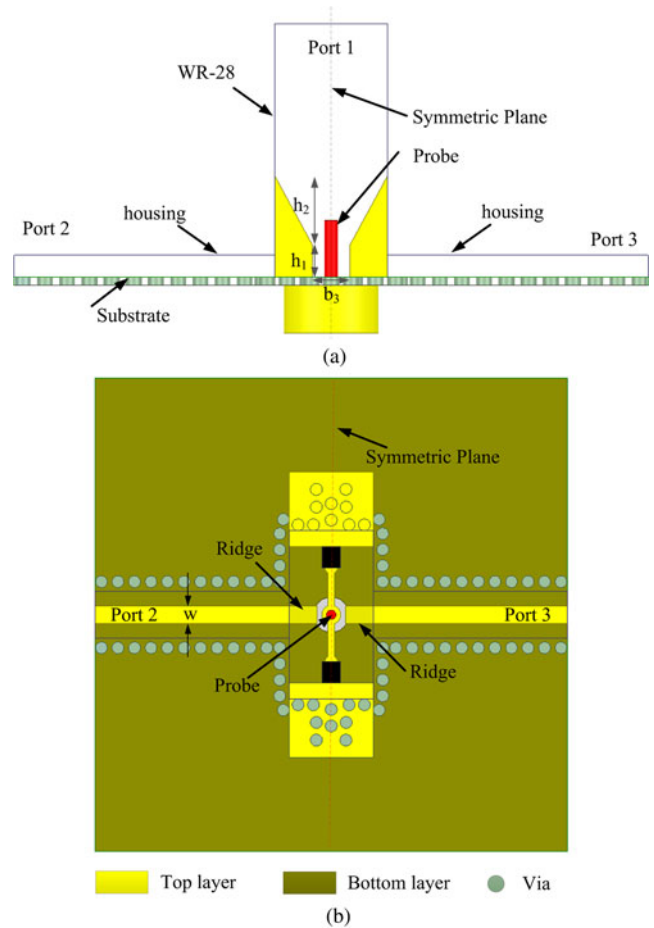

Fig. 4. Transition between waveguide and microstrip line: (a) side view and (b) top view.
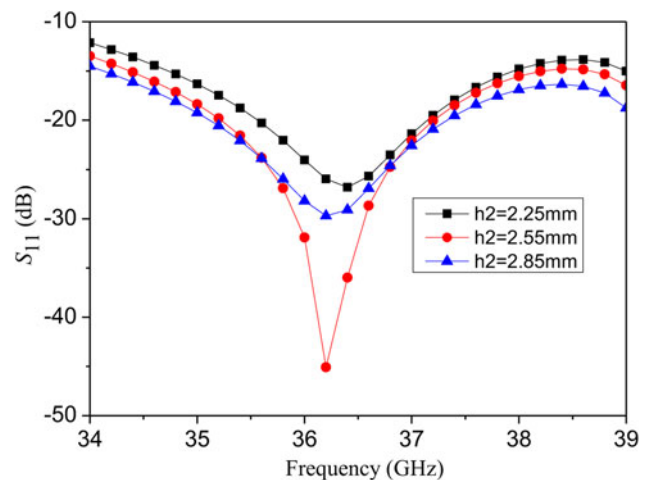
Fig. 5. Simulated results of the input return loss with varying h_2.

Isolation between two output ports

Figure 6 shows the configuration of the planar circuit and insulator. Physical dimensions of the probe are $d_1 = 0.38$ mm, $d_2 = 2.7$ mm, $l_1 = 2.04$ mm, and $l_2 = 1.5$ mm. To minimize the whole circuit, one end of the probe is cut-off when the insulator is utilized in the proposed power divider. The height of the probe (l_1) is
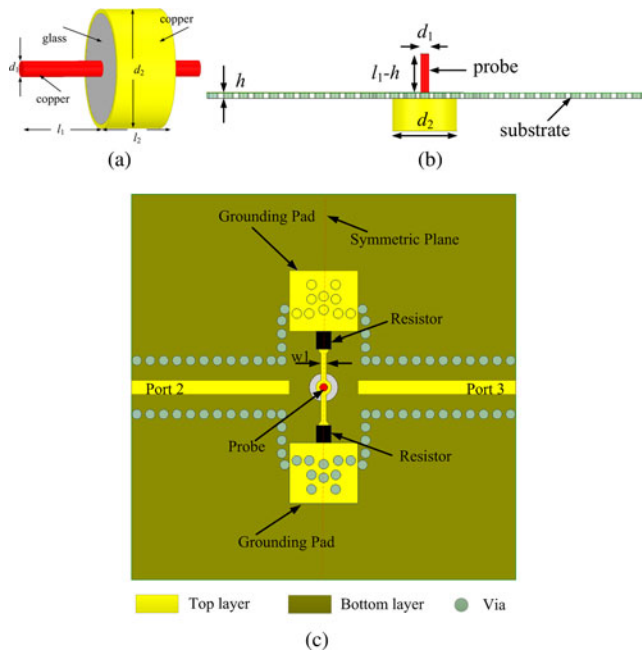
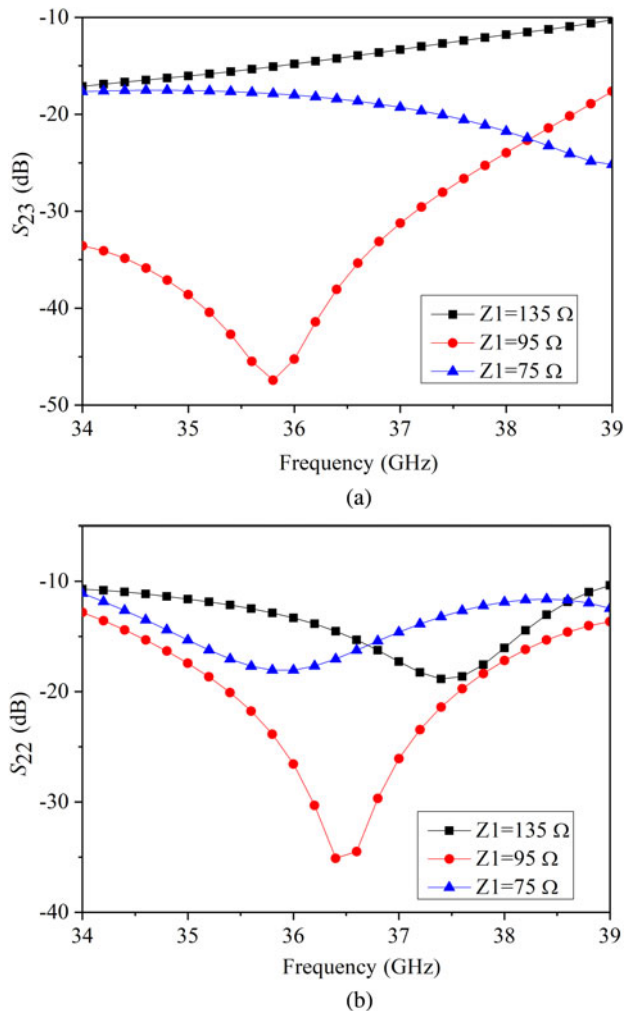**Fig. 6.** Configuration of the planar circuit and insulator: (a) insulator, (b) side view, and (c) top view.

Fig. 7. Simulated results of the power divider under different characteristic impedance: (a) S_{23} and (b) S_{22}.
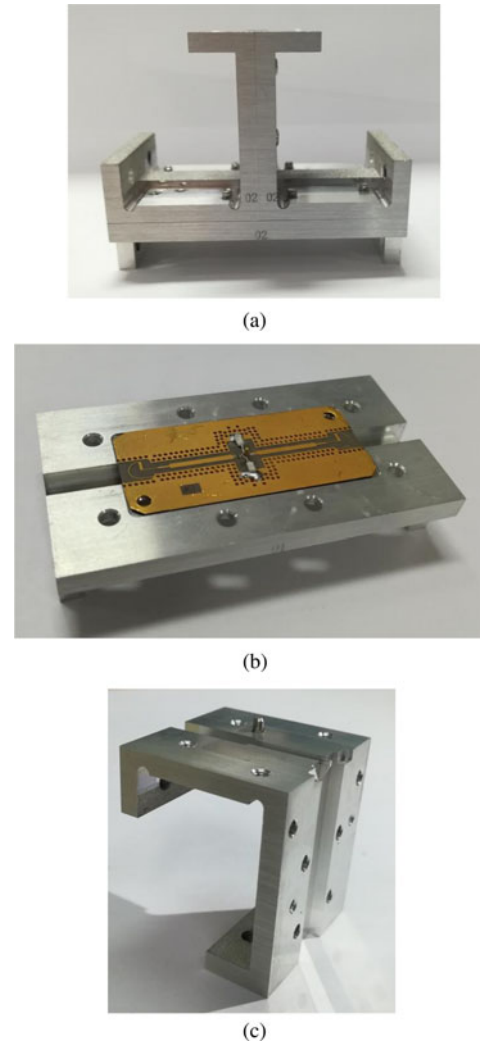

Fig. 8. Photographs of the fabricated power divider: (a) whole circuit, (b) planar circuit and bottom cavity, and (c) cavity of the left side.

about quarter-wavelength at the central operating frequency. The insulator inserts from the bottom of the substrate, as shown in Figs 6(b) and 6(c). To avoid shorting the probe, a circular metal on the backside of the substrate is removed, as shown in Fig. 6 (c). Its diameter is chosen as 1.5 mm in this proposed Ka-band power divider, which is larger than d_1 and smaller than d_2. The probe connects with the microstrip line at the top layer of the substrate. Another end of the microstrip line is connected with the chip resistor. As the chip resistor's power capacity is directly proportional to its value, the value of the chip resistor is selected as 100 Ω in this proposed circuit.

Figure 7 shows the simulated output return loss and isolation under different characteristic impedances of the microstrip line when the chip resistor's value is fixed at 100 Ω. It can be observed that the characteristic impedance has a great influence on the output return loss and isolation. This can be explained by equations (4) and (5), the output return loss and isolation are relevant with Γ_{e2} which is affected by the isolation circuit.

Since the chip resistors are mounted on the substrate and surrounded by the waveguide, physical dimensions of the chip resistor should be considered. The dimension of the standard Ka-band waveguide is 3.556 mm × 7.112 mm, and the chip resistor's
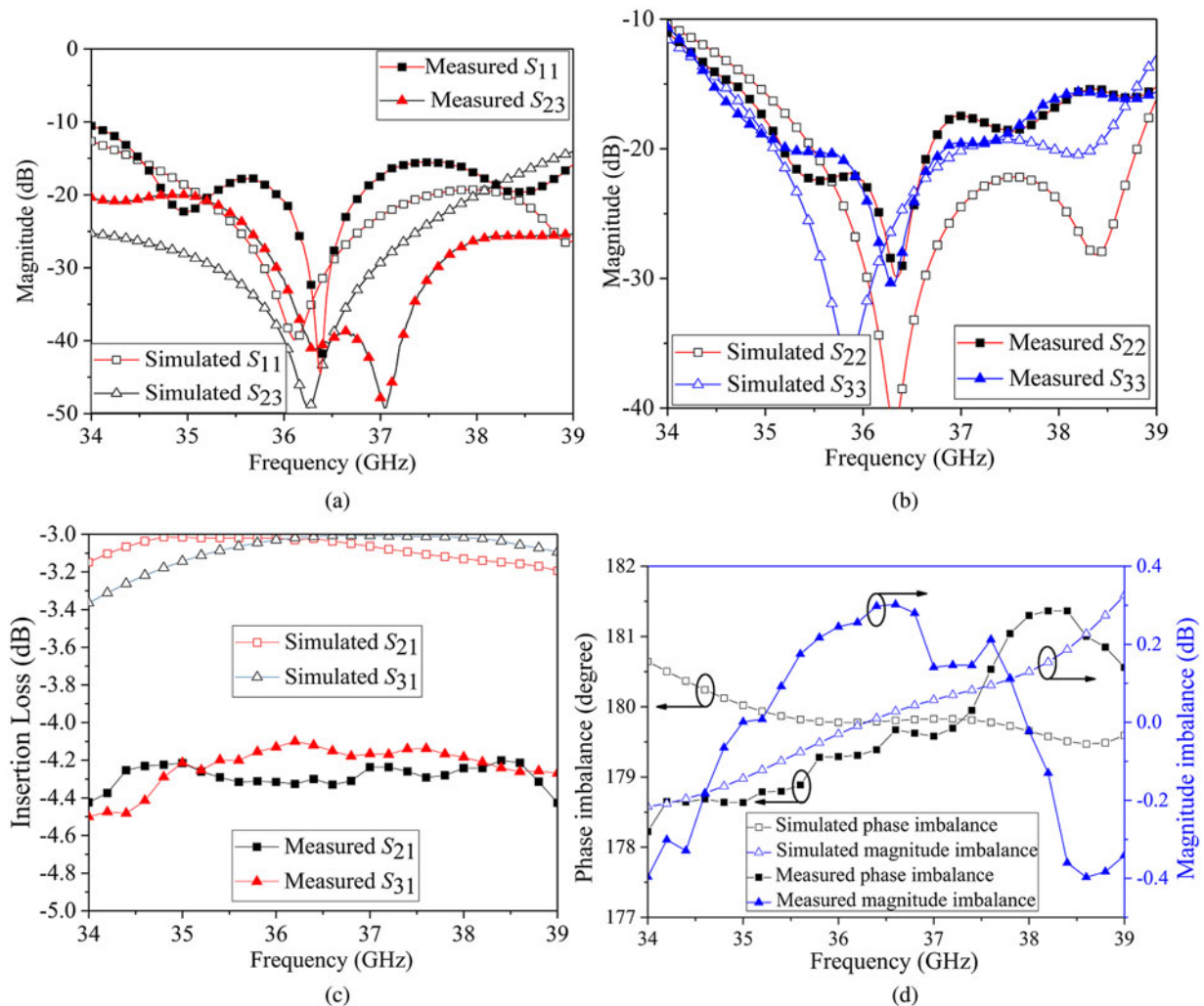
Fig. 9. Comparisons between the simulated and measured results of the proposed power divider: (a) S_{11}, S_{21}, and S_{23}, (b) S_{22} and S_{23}, (c) insertion loss, and (d) magnitude and phase imbalance.

dimension used in this circuit is $1.6\,mm \times 0.8\,mm \times 0.5\,mm$. As shown in Fig. 6(c), the total length of the microstrip line and two chip resistors may exceed the length of the waveguide (7.112 mm). Moreover, as the narrow side of the waveguide does not influence on the propagation of TE10 mode in the waveguide, two housings on the narrow side are dug to assemble the chip resistors. The dimensions of the housing are $2.5\,mm \times 2.2\,mm \times 1.5\,mm$.

Experiment and discussion

In order to validate the proposed design concept, a power divider operating at the Ka-band is simulated, fabricated, and measured. For the convenience of measurement, two microstrip-to-waveguide transitions [18] are cascaded to the planar output ports. The planar circuits are etched on the top layer of a Rogers RT/Duroid 5880 substrate. Two Vishay $100\,\Omega$ thin-film chip resistors are soldered between the microstrip line and grounding pad. The whole power divider consists of four parts, i.e. three cavities and a planar substrate. The planar substrate is sustained by the bottom cavity. Figure 8 shows photographs of the fabricated waveguide power divider. For the simplicity of fabrication, the whole cavity is divided into three parts, i.e. left-side cavity, right-side cavity, and the bottom

cavity. The left-side and the right-side cavities are symmetrical, which are bisected from the narrow side of the WR-28 waveguide.

The circuit is measured by using an Agilent N5244A network analyzer. Comparisons between the simulated and measured results are shown in Fig. 9. It can be seen that from 34 to 39 GHz, the insertion loss including waveguide-to-microstrip transition at the output port is <1.5 dB, the isolation is better than 20 dB, and the return loss of three ports is better than 10 dB. The phase deviation of two outputs is in the range of 178.3–181.3°, and the magnitude imbalance is <0.5 dB. Especially, in the range of 36.2–37.2 GHz, the isolation between two output ports are better than 40 dB, and the return loss of three ports is better than 21, 19.8, and 20.8 dB, respectively.

Table 1 shows comparisons between the proposed power divider and the previously reported ones. It can be observed that the proposed circuit has excellent isolation performance, especially when considering the isolation better than 40 dB, only the circuits in [6, 7] can achieve this level. However, their isolation bandwidths are relatively narrow. Moreover, the output ports of the circuits in [6–11, 13] are rectangular waveguide ports, which is inconvenient to integrate with other planar circuits such as power amplifiers, low noise amplifiers, and so on. Furthermore, the impedance-transformation stages in [7–11] are based on

Table 1. Comparisons between the proposed power divider and previously reported ones

Ref.	Structure	FB/f_0 (%/GHz)	IL (dB)	RL (dB)	Iso (dB)	Iso >40 dB	Amplitude/phase imbalance (dB/°)	Compact circuit size	Planar output port
[5]	SIW	40/10	3.8[a]	15	18	No	2[a]/8	Yes	Yes
[6]	Waveguide magic-T	31.6/9.5	0.4	15	22	Yes	0.12/0	Yes	No
[7]	Waveguide magic-T	21/30.75	0.2	20	20	Yes	0.25/2.5	No	No
[8]	Waveguide magic-T	18/9.25	0.2	18	16	No	±0.05/1	No	No
[9]	Waveguide T-junction	41/33.2	0.1	20	–	No	±0.03/±3.3	No	No
[10]	Waveguide T-junction	20/30	0.2	17	20	No	0.06/–	No	No
[11]	Waveguide T-junction	38/185	0.3	20	16	No	0.15/0	No	No
[12]	Waveguide T-junction	21/14.5	0.35	15	12	No	0.15/2.5	No	Yes
[13]	Waveguide	12.1/33	0.1	25	18	No	0.2/1.5	No	No
[14]	SIW 5-port Riblet	36/16.5	2	11	15	No	±0.1/±0.75	No	Yes
[15]	SIW bi-layer	25.6/9.85	0.75	10	10	No	±0.5/5	Yes	Yes
[16]	SIW bi-layer	50/12.8	0.9	10	10	No	0.3/3.7	Yes	Yes
This work	Waveguide T-junction	12/36.5	1.5[b]	10	20	Yes	(0.5/3)[b]	Yes	Yes

[a]Estimated.
[b]Including insertion loss of waveguide-to-microstrip transition at two output ports.

waveguide stepped-impedance transformers, and the isolation circuits in [7, 8, 10–13] are exposed outside. These drawbacks create a hurdle to further improve the circuit's integration level and result in a large circuit size. However, in this proposed power divider, the output ports are planar and the isolation part is hidden in the waveguide. So, it can be concluded that the proposed power divider shows advantages of compact size, planar output port, and easy integration with other circuits when compared with the power dividers in [6–11, 13]. When compared with the power dividers in [5, 8–16], the proposed power divider has the merits of high isolation.

Conclusion

A Ka-band waveguide power divider with planar output ports, compact size, and high isolation is proposed in this paper. Vertical transition between ridge waveguide and microstrip line is utilized to realize planar output ports in order to integrate with other planar circuits directly. To realize high isolation between two output ports, a probe insulator is inserted through the bottom cavity and substrate to couple the energy between two output ports, and the unwanted energy is absorbed by two chip resistors. As the ridge waveguides, probe, and chip resistors are hidden in the waveguide, so the whole circuit is very compact. For verification, a prototype power divider is simulated, fabricated, and measured. The measured results agree well with the simulated ones, which verify the validity of the proposed design concept. Comparisons between previously reported works indicate that the proposed work shows merits of waveguide power divider and SIW power divider simultaneously.

References

1. **Gupta R, Gabdrakhimov B, Dabarov A, Nauryzbayev G and Hashmi MS** (2021) Development and thorough investigation of dual-band Wilkinson power divider For arbitrary impedance environment. *IEEE Open Journal of the Industrial Electronics Society* **2**, 401–409.
2. **Nair RG and Natarajamani S** (2021) Design of Microstrip Multi-Band Resonator Power Divider. *Third International Conference on Intelligent Communication Technologies and Virtual Mobile Networks* (*ICICV*), Tirunelveli, India, pp. 656–660.
3. **Zhu H and Guo YJ** (2021) Dual-band and tri-band balanced-to-single-ended power dividers with wideband common-mode suppression. *IEEE Transactions on Circuits and Systems II: Express Briefs* **68**, 2332–2336.
4. **Liu Y, Niu D and Li ES** (2012) Three-port *E*-plane bifurcated waveguide power divider at millimeter-wave frequencies. *Asia Pacific Microwave Conference Proceedings*, Kaohsiung, Taiwan, pp. 998–1000.
5. **Pasian M, Silvestri L, Rave C, Bozzi M, Perregrini L, Jacob A and Samanta KK** (2017) Substrate-integrated-waveguide *E*-plane 3-dB power divider/combiner based on resistive layers. *IEEE Transactions on Microwave Theory and Techniques* **65**, 1498–1510
6. **Hwang KC** (2009) Design and optimization of a broadband waveguide magic-T using a stepped conducting cone. *IEEE Microwave and Wireless Components Letters* **19**, 539–541.
7. **Chu QX, Wu QS and Mo DY** (2014) A Ka-band *E*-plane waveguide magic-T with coplanar arms. *IEEE Transactions on Microwave Theory and Techniques* **62**, 2673–2679.
8. **Guo L, Li J, Huang W, Shao H, Ba T, Jiang TY, Jiang Y and Deng GJ** (2017) A waveguide magic-T with coplanar arms for high-power solid-state power combining. *IEEE Transactions on Microwave Theory and Techniques* **65**, 2942–2952.
9. **Zhao P, Wang QY, Tian X and Wang X** (2016) An integratable planar waveguide power divider with anti-phases and full bandwidth. *IEEE Microwave and Wireless Components Letters* **26**, 583–585.

10. **Xu ZB, Xu J, Cui YJ and Qian C** (2015) A novel rectangular waveguide T-junction for power combining application. *IEEE Microwave and Wireless Components Letters* **25**, 529–531.

11. **Gouda A, López CD, Desmaris V, Meledin D, Pavolotsky AB and Belitsky V** (2021) Millimeter-wave wideband waveguide power divider with improved isolation between output ports. *IEEE Transactions on Terahertz Science and Techniques* **11**, 408–416.

12. **Dang Z, Zhang Y, Zhu HL, Yan B and Xu RM** (2022) An isolated out-of-phase 3-dB power divider via waveguide-to-microstrip transition. *IEEE Microwave and Wireless Components Letters* **32**, 21–24.

13. **Ding JY, Wang QY, Zhang YB and Wang CL** (2014) A novel five-port waveguide power divider. *IEEE Microwave and Wireless Components Letters* **24**, 224–226.

14. **Huang YM, Jiang W, Jin HY, Zhou YL, Leng SP, Wang GA and Wu K** (2017) Substrate-integrated waveguide power combiner/divider incorporating absorbing material. *IEEE Microwave and Wireless Components Letters* **27**, 885–887.

15. **Djerafi T, Hammou D and Wu K** (2014) Ring-shaped substrate integrated waveguide Wilkinson power dividers/combiners. *IEEE Transactions on Microwave Theory and Techniques* **4**, 1461–1469.

16. **Vincenti Gatti R and Rossi R** (2018) Hermetic broadband 3-dB power divider/combiner in substrate-integrated waveguide (SIW) technology. *IEEE Transactions on Microwave Theory and Techniques* **66**, 3048–3054.

17. **Pozar DM**. *Microwave Engineering*, 3rd Edn. Beijing, China: Publish House of Electronics Industry, pp. 315–316.

18. **Tang C, Pan XF, Cheng F and Lin XQ** (2020) A broadband microstrip-to-waveguide end-wall probe transition and its application in waveguide termination. *Progress in Electromagnetics Research Letters* **89**, 99–104.

Cong Tang was born in Shangqiu, Henan Province, China. He received his B.S. degree in electronic engineering from PLA Information Engineering University, Zhengzhou, China in 2010, and his Ph.D. degree from the UESTC (University of Electronic Science and Technology of China), Chengdu, China in 2018. From 2020, he joined the Southwest China Institute of Electronic Technology. His research interests include millimeter-wave and microwave circuits and systems.

Xin Gao received his B.S. degree in electronic engineering from Northwest University, Xi'an, Shaanxi, China, in 1995, his M.S. degree in optics engineering from Northwestern Polytechnical University, Xi'an, in 1998, and his Ph.D. degree in optics engineering from the Xi'an Institute of Optics and Precision Mechanics, Chinese Academy of Sciences, Xi'an, in 2007. Currently, he is a Full Professor with the Beijing Institute of Tracking and Telecommunications Technology, Beijing, China. His research interests include design of satellite communication and navigation systems, and phased array signal processing.

Hongquan Zhu received his Ph.D. degree in physics engineering from Tsinghua University, Beijing, China, in 2008. Since 2008, he is with the Beijing Institute of Tracking and Telecommunications Technology and has involved in the design, construction, and maintenance of Chinese TT&C Stations. Currently, he is an Associate Professor mainly interested in millimeter-wave and microwave circuits and systems.

Jinrong Zhang received her B.S. degree and master degree in electronic engineering from the University of Science and Technology of China, Hefei, China, in 2006 and 2009, respectively. Since 2009, she is with the Beijing Institute of Tracking and Telecommunications Technology and has involved in the design, construction, and maintenance of Chinese TT&C Stations. Currently, she is an assistant Professor mainly interested in millimeter-wave and microwave circuits and systems.